

Locally Controllable Polygons by Stable Pushing

Kevin M. Lynch
 Biorobotics Division
 Mechanical Engineering Laboratory
 Namiki 1-2, Tsukuba, 305 Japan

Abstract

This paper characterizes polygons that are small-time locally controllable by stable pushing as a function of the polygon shape, the location of the center of friction, and the friction coefficient at the pushing contact. Such polygons can be pushed to follow any path arbitrarily closely, a useful property for planar manipulation. Because the pushes are stable, pushing plans can be executed without feedback.

1 Introduction and Motivation

Pushing is a useful robot primitive for manipulating large and heavy parts, parts with uncertain location, or parts that are otherwise difficult to grasp and carry. One application of pushing is parts feeding (Mani and Wilson [7]; Peshkin and Sanderson [11]; Goldberg [4]; Akella *et al.* [1]). Pushing also allows a mobile robot to easily manipulate large objects (Donald *et al.* [2]).

We are interested in characterizing the fundamental capabilities of pushing as a manipulation primitive. Toward that end we have studied the *controllability* of pushing: is it possible to push the object to the goal location? We are particularly interested in *small-time local controllability* (STLC), which implies that the object can be pushed to follow any planar path arbitrarily closely. If we have this property, we can maneuver the part in tight places.

We have previously shown that any object, other than a frictionless disk centered at its center of friction, is STLC by pushing with point contact (Lynch and Mason [6]). This implies that a two-degree-of-freedom robot (a point translating in the plane) can maneuver an object arbitrarily closely along any path in its three-dimensional configuration space $SE(2)$. (In one sense, pushing is a more complete primitive for planar manipulation than pick and place, as no frictionless disk can be rotated by grasping and turning. Pushing can rotate any frictionless disk not centered at its center of friction.)

Pushing with point contact results in unpredictable motion of the object, making planning difficult. For this reason, we have also studied *stable pushing* with line contact. A stable push is defined as a pusher contact and motion that keeps the object fixed to the pusher as it moves. Stable pushes make it possible to plan pushing paths (Figure 1) which can be executed without feedback. A pushing planner and experiments are described in (Lynch and Mason [6]).

By switching the line contacts, it is often possible to achieve STLC by stable pushing. We would like to characterize the set of polygons that are STLC by stable pushing. In this paper we give conditions for a polygon to be STLC in

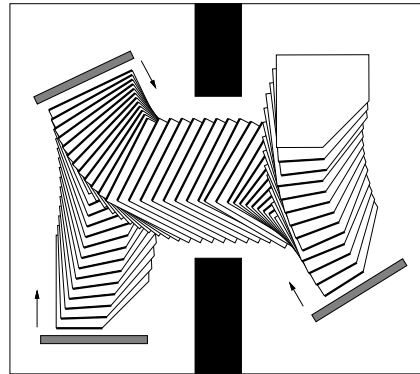


Figure 1: Maneuvering a pentagon by stable pushing with line contact. This pentagon is STLC using just the two pushing edges shown.

terms of its shape, the location of its center of friction, and the friction coefficient at the pushing contact.

By considering geometry (the shape of the polygon) and the frictional mechanics of pushing, we can demonstrate this fundamental “maneuverability” property for classes of parts by stable pushing. One aim of the science of robotic manipulation is to elucidate such characterizations of manipulation primitives. Other related results in manipulation include the demonstration of the controllability of a ball rolling on a plane or another ball (Li and Canny [5]); bounds on the number of fingers necessary for a grasp (Mishra *et al.* [9]; Markenscoff *et al.* [8]; Rimon and Burdick [12]); the classification of orientable parts by sensorless parallel-jaw grasping sequences (Goldberg [4]); and the proof that a single joint operating above a fixed-speed conveyor is sufficient to position and orient polygonal parts by pushing (Akella *et al.* [1]).

In the next section we provide definitions and a basic result used throughout the paper. Section 3 gives an algorithm for finding the minimum friction coefficient that yields STLC for a given part. Section 4 presents results on the minimum friction needed for STLC for classes of polygons. Proofs of these results are given in Section 5.

2 Definitions

The flat robot pusher is called the *pusher* and the pushed object is called the *slider*. We assume that the slider’s motion is sufficiently slow that dynamic forces are negligible compared to sliding friction. This is the *quasistatic* assumption. Pushing forces map to slider velocities, not accelerations. The state of the slider is simply its configuration \mathbf{q} .

The slider is STLC if, for any configuration \mathbf{q} of the slider

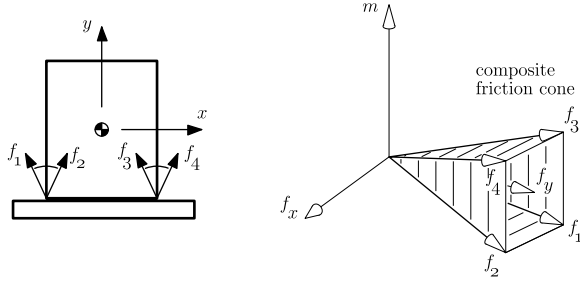


Figure 2: Friction forces through a contact edge and the representation as a convex cone in force-moment space (Erdmann [3]). Boundary forces (through an edge endpoint or at a friction boundary) are the outer “shell” and interior forces are all forces inside the shell. Forces in the $m = 0$ plane are pure forces.

and any neighborhood U of \mathbf{q} , the set of configurations the slider can reach without leaving U is a neighborhood of \mathbf{q} . By patching together these neighborhoods, the slider can follow any path arbitrarily closely. A sufficient condition for STLC of a system at a state \mathbf{q} is that the set of feasible motion directions (tangent vectors) positively spans the system’s tangent space at \mathbf{q} (Sussmann [13]). For the slider, the tangent vectors are the stable pushing directions and the tangent space is the space of all slider velocities.

We study stable pushing with line contact. The slider is a convex polygon and the pusher is a flat edge aligned with an edge of the polygon. Because the pusher is a line, non-convex polygons are equivalent to their convex hulls. The pusher can push on any edge of the slider’s convex hull.

We assume that the center of friction of the slider is in the interior of its convex hull. The planar location of the center of friction is equivalent to that of the center of mass if the support friction coefficient is uniform. We assume that only the center of friction of the slider is known; no other information about the support distribution is available.

Friction between the pusher and the slider and the support surface is assumed to conform to Coulomb’s law. At a contact, the *friction angle* α is the half-angle of the cone of forces applicable through the contact. The *friction coefficient* μ is defined $\mu = \tan \alpha$. In this paper α and μ refer to friction at the contact between the pusher and the slider.

An *interior force* for a given contact edge is defined as a force that passes through the interior of the edge at an angle less than the friction angle α . A *boundary force* is defined as a force at the friction angle α or passing through an endpoint of the edge (Figure 2). A *pure force* is a contact force through the center of friction. We will refer to *interior pure forces*, forces which are both interior and pure, and *boundary pure forces*, forces which are both on the boundary and pure. For any contact edge, the set of pure forces that can be applied is either empty, a single force direction (necessarily a boundary force), or a range of force directions (including a range of interior pure forces). The set of pure forces through an edge can be found as in Figure 3.

The velocity of the slider can be represented either as a rotation center or as a point in the three-dimensional space (v_x, v_y, ω) of velocities measured at the center of friction. Rotation centers are convenient for graphical purposes, but

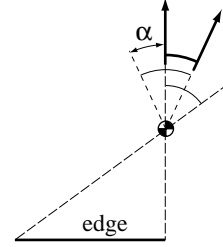


Figure 3: The cone of pure forces that can be applied through an edge is the intersection of the friction cone drawn at the center of friction and the cone formed by lines through the center of friction and the two endpoints of the edge. The boundary pure forces are the boundaries of the cone.

the three-dimensional velocity space is more convenient for proofs. A *translation* is a velocity with a zero angular component. As with forces, we can define interior and boundary velocities of a set of velocities.

In a previous paper (Lynch and Mason [6]) we described the procedure STABLE that determines a set of stable pushing motions for a given line contact, friction coefficient, and center of friction. We reproduce it in Figure 4. The pushes found by STABLE are guaranteed to be stable for the known center of friction *regardless* of the slider’s exact support distribution. We will use the following key properties of STABLE:

- If an interior pure force can be applied through the edge, then STABLE finds a set of stable pushing directions with nonempty interior including a range of translation directions aligned with the pure force directions. The stable pushing directions are a convex cone in the slider’s velocity space.
- If a single pure force can be applied, STABLE finds a single translation direction aligned with the force.
- If no pure force can be applied through the edge, then STABLE finds no stable pushing motions, and in fact it is impossible to identify any stable pushing motions without more information about the support distribution.

Using these properties of STABLE we can state the basis of the results derived in this paper.

Proposition 1 *Given a friction coefficient $\mu > 0$, the convex polygonal slider is STLC by stable pushes found by STABLE if and only if the boundary pure forces from the edge contacts positively span the plane.*

Proof: Every slider has at least one edge that can apply a set of pure forces with nonempty interior with any friction coefficient $\mu > 0$. To find such an edge, draw the maximal inscribed circle centered at the center of friction. This circle must contact an interior point of at least one edge E . The normal to E at the contact point represents a pure force, and because $\mu > 0$ and this point is interior to E , this normal corresponds to an interior pure force. Therefore a range of pure forces \mathcal{F}_E^{pure} with nonempty interior can be applied through E . STABLE finds a set of velocity directions \mathcal{V}_E

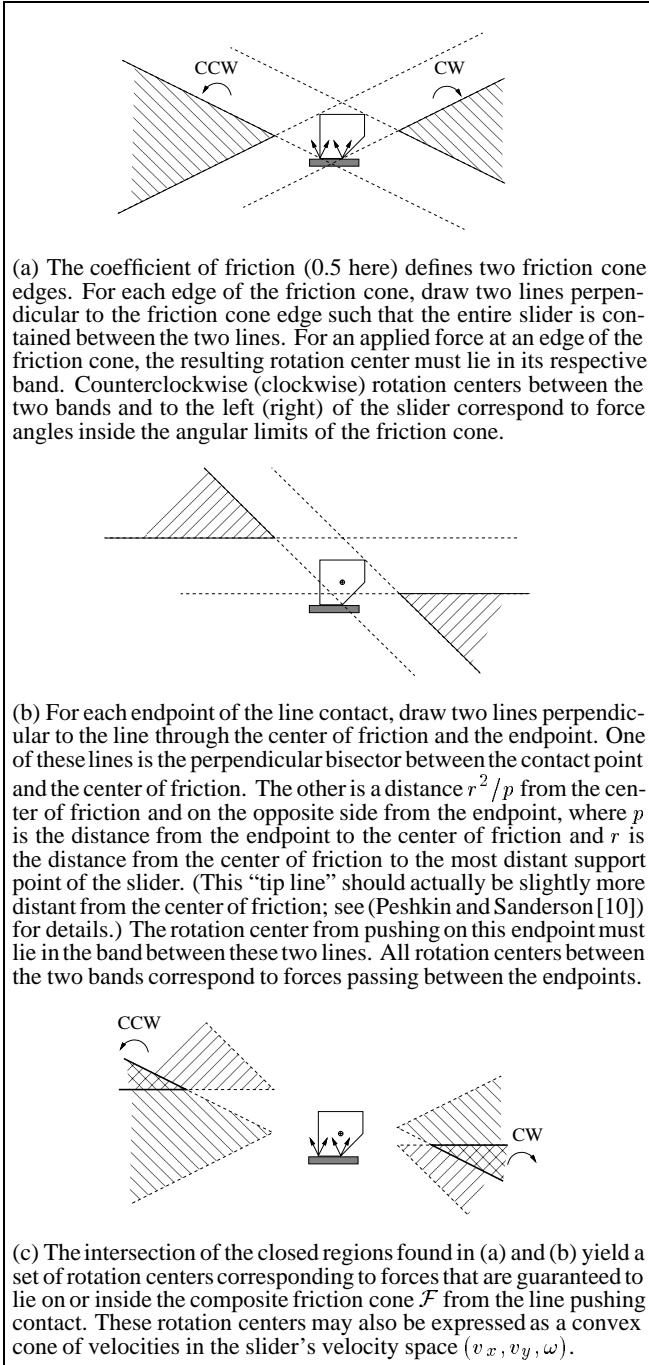


Figure 4: Procedure STABLE.

(with nonempty interior in the three-dimensional velocity space) with a set of translations \mathcal{V}_E^{trans} aligned with \mathcal{F}_E^{pure} .

For every pure force applied from every other edge, STABLE will find a translational velocity aligned with the force. The union of the boundary translations from these other edges is denoted $\mathcal{V}_{other}^{trans}$. (By convexity, it is sufficient to consider only the boundary translations.) If $\mathcal{V}_{other}^{trans}$ and \mathcal{V}_E^{trans} positively span the plane, then $\mathcal{V}_{other}^{trans}$ and $\text{int}(\mathcal{V}_E^{trans})$ also positively span the plane, where

$\text{int}(\mathcal{V}_E^{trans})$ is the set of interior translation directions of \mathcal{V}_E^{trans} . Because $\text{int}(\mathcal{V}_E^{trans})$ is interior to \mathcal{V}_E in the slider’s velocity space, \mathcal{V}_E and $\mathcal{V}_{other}^{trans}$ positively span the space of slider velocities, and the slider is STLC.

This proves that the conditions of the proposition are sufficient. To show they are necessary, assume the pure forces positively span a half-plane. Then STABLE will find a set of velocity directions confined to an open half-space \mathcal{H} , along with two opposing translations on the plane bounding \mathcal{H} . These velocities do not provide STLC (Lynch and Mason [6]).

Finally note that if $\mu = 0$, STABLE can find only translational motions, and the slider cannot be rotated by pushes found by STABLE. \square

Proposition 1 gives us a simple way to determine if a given convex polygonal slider is STLC by pushes found by STABLE for a nonzero friction coefficient μ : simply construct the boundary pure forces for each edge and check if they positively span the plane.

3 Minimum Friction Algorithm

Given a particular slider we would like to find the minimum friction coefficient μ that makes it STLC by pushes found by STABLE. Such a friction coefficient always exists. Intuitively, as we increase the friction coefficient, the set of pure forces that can be applied from each edge increases (or remains unchanged) until we hit a critical friction coefficient at which the pure forces positively span the plane. We can identify this critical value with the following steps.

1. Find the set of all critical friction angles at which the slider might become STLC. The critical friction angles are of types 1 and 2, illustrated in Figure 5.
2. Sort the corresponding critical friction coefficients $\mu = \tan \alpha$ in increasing order. Each friction coefficient should retain its type information. Remove duplicates. If there are type 1 and 2 friction coefficients with the same friction value, discard the type 2 friction coefficient.
3. Evaluate the friction coefficients until one is found which yields STLC.

Step 2 yields a sorted list of friction coefficients $(\mu_1, \mu_2, \dots, \mu_n)$, where μ_1 is always zero. To evaluate μ_i , we actually evaluate $\mu_i + \delta$, where $\delta > 0$ and $\mu_i + \delta < \mu_{i+1}$. If the boundary pure forces (Figure 3) for all edges positively span the plane for $\mu_i + \delta$, then the slider is STLC for any friction coefficient $\mu > \mu_i$. If the critical friction coefficient $\mu_i > 0$ is of type 1 in Figure 5, then if the boundary pure forces also positively span the plane for μ_i , the slider is STLC for any $\mu \geq \mu_i$.

4 Classes of Locally Controllable Polygons

Using Proposition 1 we can characterize classes of STLC polygons based on their geometry, center of friction location, and contact friction. The proofs are given in Section 5.

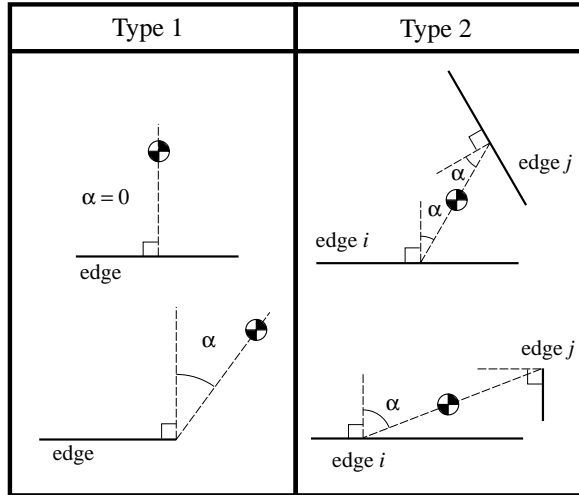


Figure 5: Critical friction angles. **Type 1:** For each edge, the critical friction angle α is the minimum friction angle such that the edge can apply a force through the center of friction. **Type 2:** For each pair of edges, the critical friction angle α is the minimum friction angle needed for the two edges to be able to apply opposite pure forces. (Some pairs of edges cannot apply opposite pure forces regardless of the friction angle. This occurs if we can draw a line through the center of friction such that both edges lie wholly on the same side of the line.)

Regular		Arbitrary	
Edges (k)	Friction (μ)	Edges (k)	Friction (μ)
5	0.325	3	0.577
7	0.228	4	1.0
9	0.176	5	1.376
11	0.144	6	1.732
13	0.121	7	2.077

Table 1: Worst-case friction coefficients for STLC for regular k -gons (k is odd) and arbitrary k -gons.

Theorem 1 (Special cases) *The convex polygonal slider is STLC by stable pushing with line contact, regardless of the location of the center of friction, if*

1. $\mu > 0$ and the slider is a rectangle, a regular $2k$ -gon ($k \geq 3$), or a triangle with all interior angles less than or equal to $\pi/2$, or
2. $\mu \geq \tan(\pi/2k)$ and the slider is a regular k -gon (k is odd, $k \geq 5$).

Theorem 2 (Number of edges) *Any convex k -gon slider is STLC by stable pushing with line contact, regardless of the location of the center of friction, if $\mu \geq \tan(\pi/2 - \pi/k)$.*

Theorem 2 implies that there exists a finite friction coefficient that yields STLC for any convex polygon. Some worst-case friction coefficients for regular k -gons and arbitrary k -gons are given in Table 1.

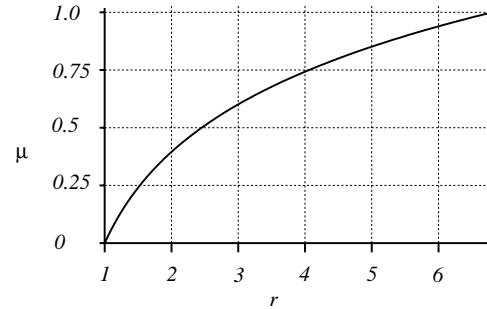


Figure 6: Worst-case friction coefficients μ for STLC as a function of the ratio r of the radius of the minimal circumscribed circle to the radius of the maximal inscribed circle.

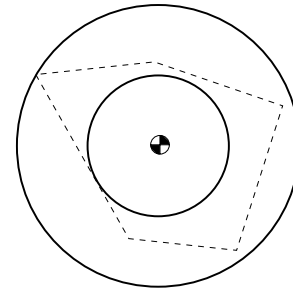


Figure 7: Any polygon with its center of friction at the point indicated and its boundary outside the inner circle and inside the outer circle ($r = 2$) is STLC by stable line contact pushes for a friction coefficient $\mu \geq 0.395$. An example polygon is shown.

The worst-case friction coefficients in Theorem 2 and part 2 of Theorem 1 require placing the slider's center of friction near a corner of the convex polygon, far from the geometric center of the slider. Thus another useful characterization of polygons is based on the location of the center of friction.

Theorem 3 (Center of friction location) *Draw the largest inscribed circle and smallest circumscribed circle centered at the center of friction. The radius of the inscribed circle is a and the radius of the circumscribed circle is ra ($r > 1$). Then r and the worst-case friction angle α are related by $r = \sec(\alpha)e^{\frac{\pi}{2}\tan\alpha}$. If $\mu \geq \tan\alpha$, the slider is STLC by stable pushing with line contact.*

Figure 6 shows a plot of the worst-case friction coefficient for STLC as a function of the ratio r . Figure 7 illustrates Theorem 3 for the case $r = 2$.

5 Proofs

Edges of a k -gon slider are numbered $1 \dots k$ in a counterclockwise fashion. Vertices are also numbered $1 \dots k$ counterclockwise such that edge 1 is bounded by vertices 1 and 2 and edge k is bounded by vertices k and 1. The interior angle between 2 adjacent edges is defined as in Figure 8.

5.1 Theorem 1

1. If the slider is a rectangle or a triangle with all interior angles less than or equal to $\pi/2$, then the perpendicular projection of each edge contains the entire interior of the slider.

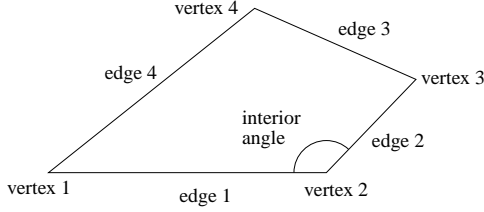


Figure 8: Polygon definitions.

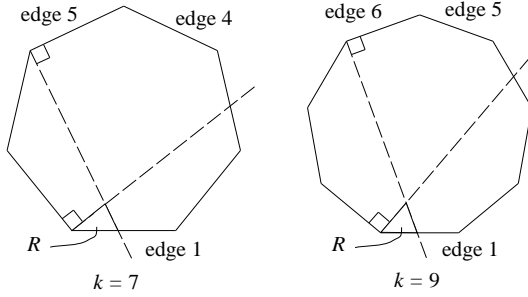


Figure 9: The region R and its construction.

Therefore each edge can apply a pure force through the center of friction, and these pure forces positively span the plane. If the friction coefficient μ is nonzero, then the slider is STLC by Proposition 1.

For a regular $2k$ -gon, $k \geq 3$, there are always two opposing edges with opposing interior normals that pass through the center of friction regardless of its location. If $\mu > 0$, then pure forces from these two edges positively span the plane, and the slider is STLC from these two edges. To find two such edges, draw the largest inscribed circle centered at the center of friction. Any edge that contacts the circle, along with its opposing edge, are sufficient for STLC.

2. A regular k -gon slider (k is odd, $k \geq 5$) is STLC for any $\mu > 0$ and center of friction placement other than in one of $2k$ triangular regions near the vertices of the k -gon. Without loss of generality, consider the triangular regions R illustrated in Figure 9. For a center of friction in R , only normals to edge 1 and edge $(k+1)/2$ pass through the center of friction. Since these edges are not opposite, they are not sufficient for STLC for all $\mu > 0$.

Increasing the friction coefficient, the slider first becomes STLC using only edges 1 and $(k+3)/2$ for all centers of friction in R . To find the required friction angle, draw the line segment C connecting vertex 1 and vertex $(k+5)/2$ (Figure 10). The friction angle is just the angle of C relative to the normals of the 2 edges, $\pi/2k$. At this friction angle, pure forces from edges 1 and $(k+3)/2$ positively span the plane for any center of friction location in R .

5.2 Theorem 2

Assume the center of friction of the slider is at $(-\epsilon, \epsilon)$ ($\epsilon > 0$) and edge 1 of the slider is aligned with the x axis, stretching from $(-\infty, 0)$ to $(0, 0)$. Edge 2 is at an interior angle of $\pi - 2\pi/k$ with respect to edge 1 and has length d . Edge n , $n = 3 \dots k$, is at an angle $\pi - \pi/k$ with respect to edge $n-1$ with length d^{n-1} (except edge k , which has infinite length;

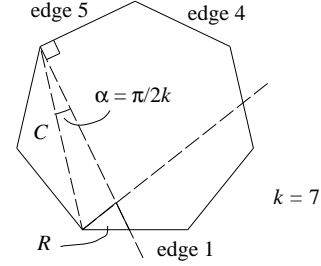


Figure 10: Determining the worst-case friction angle.

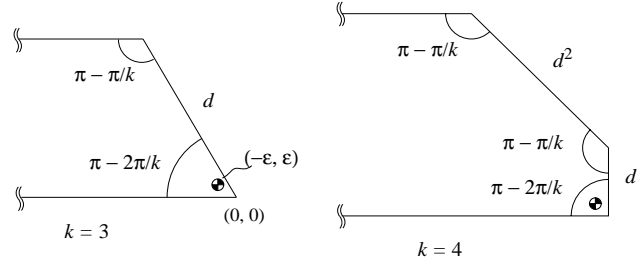


Figure 11: As $\epsilon \rightarrow 0$ and $d \rightarrow \infty$, these polygons require the worst-case friction coefficient for STLC.

see Figure 11). Edge 1 and edge k are parallel and meet at infinity with zero interior angle. (To be an actual polygon, of course, these edges cannot be exactly parallel, but here we consider the limiting case.) As ϵ approaches zero and d goes to infinity, the friction angle required to make the slider STLC goes to $\pi/2 - \pi/k$. With this friction angle, all edges can apply a pure force, and the slider is STLC. At any smaller friction angle, it is possible to choose ϵ and d so that only edges 1 and 2 can apply pure forces. The positive span of these forces is confined to an open half-plane, and the slider is not STLC.

When the friction angle is increased to $\pi/2 - \pi/k$, the friction forces through edge n ($n \geq 3$) include a force along edge $n-1$. As $\epsilon \rightarrow 0$ and $d \rightarrow \infty$, this force approaches the pure force from edge n through the center of friction.

The detailed proof that a k -gon slider of this type requires the largest friction coefficient of all k -gons is somewhat laborious. Simply stated, if we try to design a polygon which requires a friction coefficient larger than $\pi/2 - \pi/k$, we find that the polygon cannot be closed with only k edges. The sliders described here are designed so as friction increases from zero, pure forces are confined to a half-plane until friction has been increased so high that, simultaneously, pure forces can be applied from all edges.

5.3 Theorem 3

To investigate the limiting behavior, we allow the slider to be any closed convex curve. This curve can be approximated arbitrarily closely by a polygon.

The problem is: given a friction angle α , find the slider that 1) is marginally STLC and 2) minimizes the ratio r of the radius ra of the circumscribed circle to the radius a of the inscribed circle. This is equivalent to maximizing the friction coefficient necessary for STLC for a slider with ratio r . Without loss of generality, assume $a = 1$.

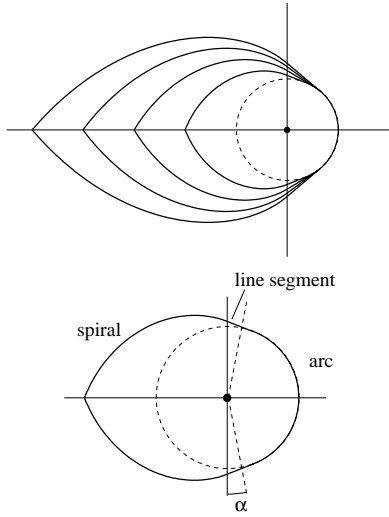


Figure 12: Examples of sliders that maximize the required friction coefficient for STLC for $r = 2, 3, 4, 5$. The pieces of the slider are shown for $r = 2$.

The solutions for several different values of α are shown in Figure 12. Each slider consists of a circular arc, two spiral curves, and two line segments connecting the circular arc to the spiral curves. The circular arc is centered at the origin (the center of friction), has unit radius, and sweeps the angle from $-\pi/2 + \alpha$ to $\pi/2 - \alpha$. The two line segments are tangent to the ends of the arc and connect to $(0, \sec \alpha)$ and $(0, -\sec \alpha)$. The arc and line segments provide pure forces which positively span a half-plane. From there, the curve spirals away from the center of friction such that the tangent of the curve at every point is at an angle $\pi/2 + \alpha$ to the line connecting the curve to the center of friction. Thus, along the spiral segments, only boundary friction forces pass through the center of friction.

To find the top spiral, we solve the differential equation

$$ds = s d\theta \tan \alpha$$

where (s, θ) is the polar representation of the spiral (Figure 13). Rearranging

$$\frac{ds}{s} = d\theta \tan \alpha$$

and integrating, we get

$$\ln s - \ln s_0 = (\theta - \theta_0) \tan \alpha,$$

where (s_0, θ_0) is the start point of the spiral. Exponentiating and rearranging, we get

$$s = s_0 e^{(\theta - \theta_0) \tan \alpha}.$$

Plugging in $s_0 = \sec \alpha$, $\theta_0 = \pi/2$, and the end angle $\theta = \pi$, we calculate r :

$$r = \sec(\alpha) e^{\frac{\pi}{2} \tan \alpha}.$$

This curve is guaranteed to give the smallest possible value of r while keeping pure forces on the boundary. Furthermore, the arc and line segments minimize the value of

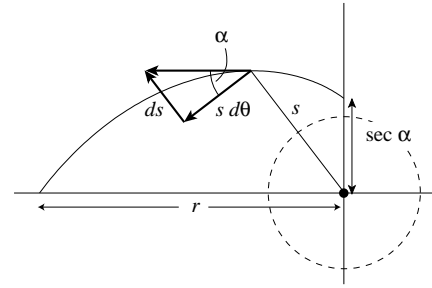


Figure 13: Constructing the spiral segment.

s_0 while confining pure forces to a half-plane. Therefore, this slider minimizes r for a given α ; equivalently, this slider maximizes the required friction angle α for a given r .

This slider is only marginally STLC for the friction angle α . For any friction angle less than α , we can find a polygonal approximation to the slider that is not STLC. In particular, we can choose a piecewise linear approximation to the spiral such that no pure forces can be applied through it.

6 Conclusion

By considering the part's geometry and frictional properties, this paper has characterized parts that can be maneuvered closely along arbitrary paths by open-loop stable pushing. These results help further establish the theoretical scope of pushing as a manipulation primitive.

References

- [1] S. Akella, W. Huang, K. M. Lynch, and M. T. Mason. Planar manipulation on a conveyor with a one joint robot. In *International Symposium on Robotics Research*, pages 265–276, 1995.
- [2] B. R. Donald, J. Jennings, and D. Rus. Information invariants for cooperating autonomous mobile robots. In *International Symposium on Robotics Research*, 1993. Cambridge, Mass: MIT Press.
- [3] M. A. Erdmann. On a representation of friction in configuration space. *International Journal of Robotics Research*, 13(3):240–271, 1994.
- [4] K. Y. Goldberg. Orienting polygonal parts without sensors. *Algorithmica*, 10:201–225, 1993.
- [5] Z. Li and J. Canny. Motion of two rigid bodies with rolling constraint. *IEEE Transactions on Robotics and Automation*, 6(1):62–72, Feb. 1990.
- [6] K. M. Lynch and M. T. Mason. Stable pushing: Mechanics, controllability, and planning. *International Journal of Robotics Research*, 15(6):533–556, Dec. 1996.
- [7] M. Mani and W. Wilson. A programmable orienting system for flat parts. In *North American Manufacturing Research Institute Conference XIII*, 1985.
- [8] X. Markenscoff, L. Ni, and C. H. Papadimitriou. The geometry of grasping. *International Journal of Robotics Research*, 9(1):61–74, Feb. 1990.
- [9] B. Mishra, J. T. Schwartz, and M. Sharir. On the existence and synthesis of multifinger positive grips. *Algorithmica*, 2(4):541–558, 1987.
- [10] M. A. Peshkin and A. C. Sanderson. The motion of a pushed, sliding workpiece. *IEEE Journal of Robotics and Automation*, 4(6):569–598, Dec. 1988.
- [11] M. A. Peshkin and A. C. Sanderson. Planning robotic manipulation strategies for workpieces that slide. *IEEE Journal of Robotics and Automation*, 4(5):524–531, Oct. 1988.
- [12] E. Rimon and J. W. Burdick. New bounds on the number of frictionless fingers required to immobilize planar objects. *Journal of Robotic Systems*, 12(6):433–451, 1995.
- [13] H. J. Sussmann. A sufficient condition for local controllability. *SIAM Journal on Control and Optimization*, 16(5):790–802, Sept. 1978.